ChemComm

ROYAL SOCIETY OF CHEMISTRY

FEATURE ARTICLE

View Article Online
View Journal | View Issue

Cite this: *Chem. Commun.*, 2025, **61**, 17544

Recent advances in using strong-field ancillary ligands to support blue-emitting iridium(III) and platinum(II) complexes

Son N. T. Phan, Ngoc B. Nguyen and Thomas S. Teets *

The design of blue-phosphorescent metal compounds with high photoluminescence (PL) quantum yields, good color purity, short PL lifetimes, and good photostability has long been a significant challenge. Strong-field ancillary ligands are widely employed to destabilize the deleterious metal-centered (^{3}MC) states and access high-performing blue-phosphorescent iridium and platinum complexes. These materials are attractive for various optoelectronic applications, most prominently organic light-emitting diodes (OLEDs). This review highlights our work and other groups' recent research on blue-emitting Ir(III) and Pt(II) phosphors incorporating strong-field ligands, and provides an outlook on the future of this field. Isocyanides, cyanide (free or terminated by a Lewis acid), and N-heterocyclic carbenes (NHCs) are all highlighted as common classes of strong-field ligands used to improve blue phosphorescence. Each of these ligand classes offers distinct advantages in the design of blue phosphors, which are highlighted in this work. NHCs are inherently strong donors with well-established synthetic chemistry with 5d metals, and when used as cyclometalating ligands they impart larger HOMO–LUMO gaps than most other classes of cyclometalating ligands. Cyanides and isocyanides are reasonably strong σ donors and good π acceptors, and both can be functionalized to further improve blue-phosphorescence metrics. In particular, isocyanides can be converted to acyclic diaminocarbenes by nucleophilic addition, even stronger σ-donating ligands than NHCs, and our group's efforts to install ADCs and further enhance the PL quantum yields of blue emitters are described.

Received 24th April 2025,
Accepted 13th October 2025

DOI: 10.1039/d5cc02300a

rsc.li/chemcomm

Department of Chemistry, University of Houston, 3585 Cullen Blv. Room 112, Houston, TX 77204-5003, USA. E-mail: tteets@uh.edu

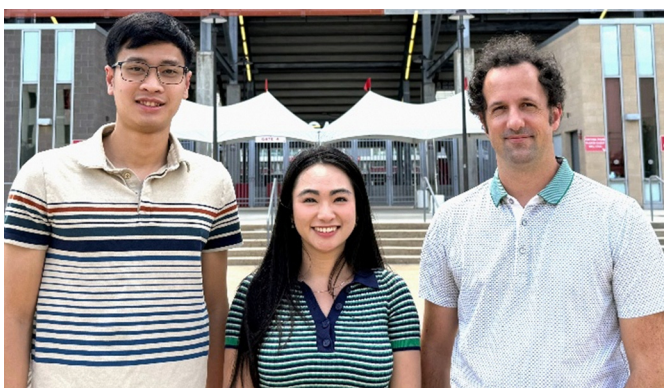

Left to right: Son N. T. Phan, Ngoc B. Nguyen, and Thomas S. Teets

Son N. T. Phan earned his BEng degree from Ho Chi Minh City University of Technology in Vietnam, where he did research in synthetic organic chemistry. He enrolled as a PhD student at the University of Houston in 2023 and is currently a third-year graduate student. Ngoc B. Nguyen, also originally from Vietnam, completed a BS in biochemistry at the University of Houston and remained there to pursue a PhD degree in chemistry, where she is likewise in the third year of study. Son and Ngoc are both researchers in the group of Prof. Thomas S. Teets, currently the Russell A. Geanangel Prof. of Chemistry at the University of Houston. Prof. Teets earned a BS degree from Case Western Reserve University, followed by a PhD at Massachusetts Institute of Technology and postdoctoral research at California Institute of Technology, before starting his independent career in 2014. He leads a physical inorganic chemistry research group that focuses mainly on the photochemistry and photophysics of coordination compounds and organometallic complexes, emphasizing photosensitizers for photoredox catalysis and phosphorescent compounds for optoelectronic applications.

Introduction

Fundamentals and applications of phosphorescence

Photoluminescence (PL) is a process by which an electronically excited molecule or material decays to the ground state *via* emission of a photon. For molecular compounds there are two main mechanisms for luminescence. When the involved excited state is the same spin multiplicity as the ground state, it is termed ''fluorescence,'' whereas luminescence that occurs from an excited state with a different spin multiplicity than the ground state is termed ''phosphorescence'', which will be the focal point of this article. Most phosphorescent molecules have closed–shell, singlet ground states, such that phosphorescence represents radiative decay from a triplet excited state back to the ground state. Fundamental aspects of phosphorescence have been actively researched for decades, and the topic has received broad interest in the chemistry community and beyond, due to the applications of phosphorescent compounds in many areas, including optoelectronics,[1–3] photocatalysis,[4–6] photosensing,[7–9] and bio-imaging.[10–12]

For most applications of phosphorescent metal complexes, there are three key measurables that need to be considered to determine if a compound is suitable for that application. The first is the spectral profile, which is the intensity *vs.* wavelength profile that a phosphorescent molecule produces, *i.e.*, the color of the emitted light. At a simple level, this color profile is determined by the energy gap between the ground state and triplet excited state that generates the phosphorescence. The other two common measurables, photoluminescence quantum yield (Φ_{PL}) and lifetime (τ), depend on the kinetics of the decay from the excited state to the ground state. When an excited molecule decays, it produces photons with a first-order radiative rate constant, abbreviated as k_r. There are also one or more nonradiative pathways that lead to excited-state decay *via* thermal processes, without generating a photon. Their combined rate constant is referred to as the nonradiative rate constant, k_{nr}. The four parameters outlined above are related by the following equations:

$$\Phi_{PL} = \frac{\#\text{ of emitted photons}}{\#\text{ of absorbed photons}} = \frac{k_r}{k_r + k_{nr}}; \tau = \frac{1}{k_r + k_{nr}}$$

The PL quantum yield (Φ_{PL}) is an efficiency metric defined as the number of emitted photons over the number of absorbed photons. For most applications of photoluminescent compounds, it is desirable to maximize Φ_{PL}, which is achieved by some combination of large k_r and small k_{nr} values.[13] The optimum lifetime depends on the chosen application. For applications like sensing that involve a phosphorescent molecule reacting with an analyte in solution, long τ values are preferred. In contrast, for many optoelectronic applications like organic light-emitting diodes, short τ values are desirable to maintain high efficiency over a wide range of brightness.

Phosphorescent Ir(III) and Pt(II) complexes

Phosphorescent iridium(III) and platinum(II) complexes have been heavily researched in fundamental and applied settings. These metals promote fast radiative decay from the triplet state to the ground state,[14–16] often leading to phosphorescence with high quantum yields and comparatively short lifetimes (μs range). In addition, like all phosphorescent compounds, Ir(III) and Pt(II) complexes allow the harvesting of both singlet and triplet excitons in organic light-emitting diodes (OLEDs), which leads to higher theoretical and practical device efficiencies. These combined attributes of Ir(III) and Pt(II) phosphors make them ideal candidates for OLED applications.[17–20] In the context of color displays, OLEDs that produce the three primary colors (red, green, and blue), have been fabricated using Ir(III) and Pt(II) dopants, with early works dating back to over 20 years ago.[21–28] Whereas green and red Ir(III) phosphors have been commercialized, the discovery of any blue-phosphorescent compound that is both efficient and stable enough to be commercialized remains a significant challenge. This challenge is described more specifically later.

Structural classes and PL profiles

Before describing the fundamental challenges associated with efficient and stable blue phosphorescence, this section outlines the structural classes of blue-phosphorescent compounds that are the focus of this review. In general, Ir(III) complexes with d^6 electronic configuration adopt an octahedral six-coordinate geometry, while the d^8 configuration of Pt(II) complexes leads to four-coordinate, square planar geometries. These complexes could either be charge-neutral or ionic, yet the former is preferable for OLED fabrication.[29] In both classes of compounds, combinations of bidentate and monodentate ligands are most commonly employed, although ligands with higher denticities have found success as well. In heteroleptic structures, the ligand that is primarily responsible for the PL color profile of a complex is often termed as the ''chromophoric'' or ''main'' ligand. These are often bidentate cyclometalating ligands (denoted as C^Y), consisting of a metalated aryl ring (C) and an N-heterocycle or N-heterocyclic carbene neutral donor (Y). In one prominent class of blue-phosphorescent platinum complexes, aryl acetylides can also be employed as chromophoric ligands.[30,31] The remainder of the coordination sphere in heteroleptic complexes is occupied by one or more ancillary ligands, which can have a large effect on the PL decay dynamics (k_r and k_{nr}) and Φ_{PL}, but usually only have subtle effects on the PL profile.[32–34] The structural classes of Ir(III) and Pt(II) complexes that are the subject of this review are displayed in Fig. 1.

Homoleptic cyclometalated complexes of both Ir(III) and Pt(II) have been long known[35,36] and the Ir(III) analogues have remained prominent in the context of blue phosphorescence and blue OLEDs.[37–43] That said, heteroleptic complexes containing both chromophoric ligands and ancillary ligands are often synthetically simpler, and the ancillary ligands provide an additional layer of control over the photophysical properties. The work from our group highlighted here focuses on heteroleptic Ir(III) complexes containing two cyclometalating ligands coupled with one bidentate or two monodentate ancillary ligands.[44–52] There are, however, a wide range of structure types investigated by other groups, including heteroleptic Ir(III) complexes with two

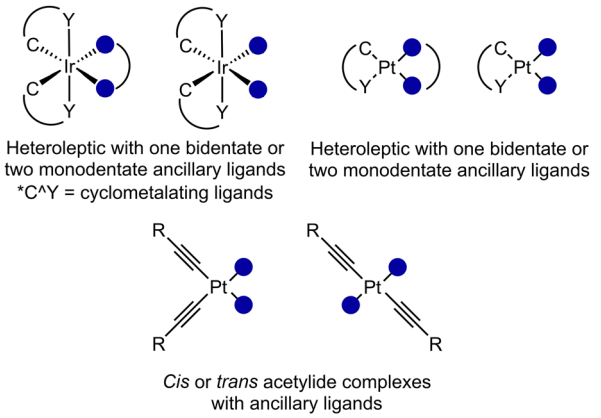

Fig. 1 Major classes of blue-emitting complexes that are the focus of this review.

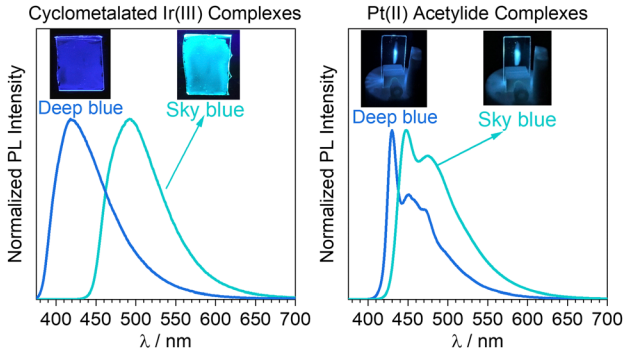

Fig. 2 Representative PL spectra of cyclometalated iridium(III) complexes (left) and platinum(II) acetylide complexes (right) with deep-blue and sky-blue luminescence. The insets show photographs of PMMA films of the compounds under UV irradiation. The PL spectra are for complexes **23**, **24**, **57**, and **58**, described later in this article.

pincer tridentate ligands[53–56] and others.[57–62] Regarding platinum complexes, this article describes monometallic Pt(II) compounds containing a cyclometalating ligand and two monodentate ancillary ligands,[63,64] and Pt(II) bis(acetylide) complexes which can adopt either *cis* or *trans* coordination modes.[65–68] Some other common structure types studied by other groups are tridentate or tetradentate Pt(II) complexes,[69–73] and dimeric Pt(II) complexes where the close approach of the two metals is important for their PL.[74–76]

The PL profiles of blue-phosphorescent Ir(III) and Pt(II) complexes can be engineered through the modification of the cyclometalating or acetylide ligands. To achieve blue phosphorescence, large HOMO–LUMO gaps are needed, to give triplet excited states that are high enough in energy to produce blue photons upon radiative decay to the ground state. Extensive research has been conducted on the design of cyclometalating ligands, coordinating through a carbon atom and a nitrogen atom (C^N type) or two carbon atoms (C^C type). Some strategies to engender blue phosphorescence include introducing strong electron-withdrawing groups to stabilize the highest occupied molecular orbital (HOMO) and/or strong electron-donating groups to destabilize the lowest unoccupied molecular orbital (LUMO).[25] Cyclometalating ligands of this type are well suited for both Ir(III) and Pt(II) complexes. Acetylides, on the other hand, are rarely studied in Ir(III) compounds, but more commonly in Pt(II) complexes.[31,77] Introducing electron-donating or electron-withdrawing groups on phenylacetylide derivatives could enable color tuning of Pt(II) acetylide complexes.[66,78] Compared to the C^N type cyclometalating ligands, NHC-based C^C ligands usually engender deeper-blue PL,[29] while an attractive feature of aryl acetylides is that they can yield sharper PL bands.[30] The photoluminescence spectra shown in Fig. 2 below illustrate typical sky-blue and deep-blue PL profiles, from representative examples of cyclometalated Ir(III) and Pt(II) acetylide complexes discussed later in this article.

The color purity of blue phosphorescence is an important criterion when selecting complexes to fabricate OLED devices for color displays. Qualitatively, the shade of the emitted blue light is often bifurcated and described as either sky blue or deep blue. The more rigorous and quantitative method to evaluate color purity is with Commission Internationale de L'Eclairage (CIE) coordinates, which converts the spectral profile into a two-dimensional, (x,y) color plot. Sky-blue and deep-blue emitters are often defined as possessing CIEy < 0.40 and 0.15, respectively.[80,81] In addition, there are more rigorous industry standards that define ideal CIEy values for deep-blue color; all of them recommend CIE < 0.1 for deep-blue phosphorescence. For example, CIEy = 0.06 for the International Electrotechnical Commission (IEC) sRGB standard, CIEy = 0.08 for the National Television System Committee (NTSC), and CIEy = 0.07 for the Society of Motion Picture and Television Engineers (SMPTE-C).[50] In color displays, deeper-blue emitters are more desirable than sky-blue analogues due to their ability to give a wider color gamut and higher color purity, although sky-blue devices usually have higher efficiency and longer device lifetimes.[80]

Challenges and the role of strong-field ancillary ligands

As described above, achieving a high Φ_{PL} requires a fast radiative rate (large k_r value) and a slow nonradiative rate (small k_{nr} value). The radiative rate constant is strongly dependent on the spin–orbit coupling in the excited state, which is proportional to the fourth power of the atomic number of the metal center.[14,15] As a result, iridium and platinum complexes tend to have comparatively large k_r values. However, spin–orbit coupling is also dependent on the coordination geometry, which influences valence d-orbital splitting, and as such is much larger in d^6 octahedral Ir(III) compounds, resulting in large k_r values. The less effective SOC in d^8 Pt(II) complexes results in smaller k_r values.[15]

Although k_r must be considered, in blue-phosphorescent compounds, the most significant challenge has been to suppress the inherently fast nonradiative decay. The triplet excited state from which phosphorescence originates (abbreviated as T_1) is usually a combination of triplet ligand-centered (^{3}LC, or $^3(\pi \rightarrow \pi^*)$) states and triplet metal-to-ligand charge transfer (^{3}MLCT, or $^3(d \rightarrow \pi^*)$) states, which both involve the conjugated ligands. Because blue phosphorescence requires a high-energy T_1 state, thermal population of higher-lying and nonradiative triplet

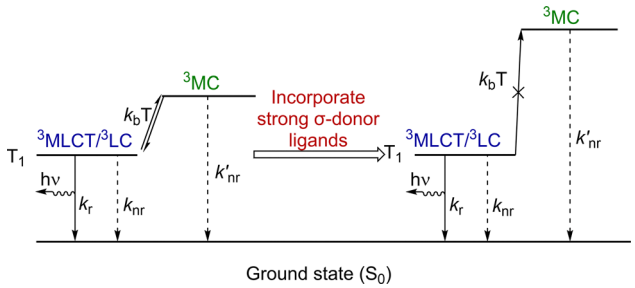

Fig. 3 Simplified excited-state diagram showing the effect of strong σ-donating ancillary ligands in destabilizing triplet metal-centered excited states.

metal-centered d–d (^{3}MC) excited states is possible, resulting in an increase in k_{nr} value.[15,29] This thermal population becomes more problematic as the PL is shifted deeper into the blue region. Population of ^{3}MC states also leads to poor stability in many blue-phosphorescent compounds, since ligand dissociation is facile once the ^{3}MC states are accessed.[82–84] As illustrated in Fig. 3, a solution to this is to incorporate strong-field ligands into blue-emitting complexes, which is most effective when the ligands are strong donors.[51] These ligands increase the energy gaps between the transition metal d orbital energy levels (*i.e.*, the ligand field splitting), thus destabilizing the ^{3}MC excited states to suppress their thermal population and allowing efficient phosphorescence from the T_1 state.[15] This strategy has been widely applied to reduce the k_{nr} value in blue-phosphorescent complexes and is the major focus of this review.

Common strong σ-donating ancillary ligands are presented in Fig. 4, including isocyanides, cyanide, and N-heterocyclic carbenes (NHCs). The carbene ligand classes generally possess strong σ-donating and weak π-accepting abilities, whereas isocyanides and cyanide are not as strong σ donors but are strong π acceptors.[85–87] In many classes of compounds, NHC-based cyclometalating ligands, such as *N*-phenylimidazol-2-ylidene-based derivatives, act as the chromophoric ligands to give deep-blue luminescence.[30,37] Acyclic diaminocarbenes (ADCs) represent an alternative class of strong donors for designing blue emitters (Fig. 4). In comparison with NHCs, ADCs have stronger σ-donating ability on account of the larger N–$C_{carbene}$–N angles (close to 120° in ADCs *versus* about 105° in NHCs). This renders more 2p character into the $C_{carbene}$ donor orbital of the ADC, facilitating stronger overlap with the metal σ* acceptor orbital (Fig. 5) and better σ donation.[88,89] Our group has pioneered the use of ADCs as ancillary ligands to produce top-performing blue-emitting Ir(III) and Pt(II) complexes, which will be discussed in this review.

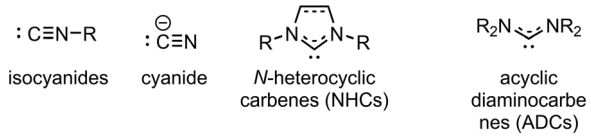

Fig. 4 Common strong σ donors used as ancillary ligands in blue-emitting complexes.

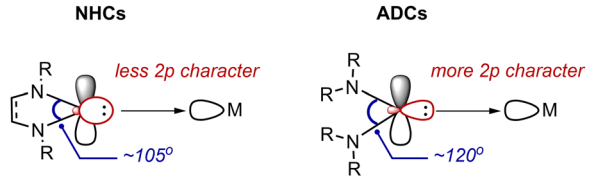

Fig. 5 Comparison between NHC and ADC ligands.

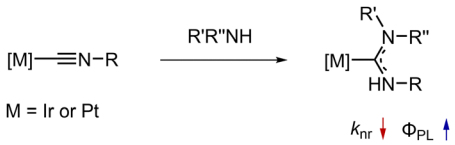

Scheme 1 Metal-mediated nucleophilic addition to isocyanide strategy to synthesize acyclic diaminocarbenes in Ir(III) and Pt(II) complexes used by our group.

There are different synthetic methods to prepare metal–ADC complexes, including lithium–halogen exchange, direct complexation, oxidative addition, and metal-mediated addition.[88] The last strategy, which is based on the metal-mediated nucleophilic addition to isocyanides, has been extensively employed by our group and others in preparing Ir(III) and Pt(II) complexes. The ADCs that thus form, being much stronger donors than isocyanides, typically reduce k_{nr} and increase Φ_{PL} relative to the isocyanide precursor (Scheme 1). This method also features mild reaction conditions and simple work-up and purification.

Outline and scope of article

This Feature article provides an overview of research conducted by our group and other groups in employing strong-field ancillary ligands to support blue-phosphorescent Ir(III) and Pt(II) complexes. The ancillary ligand classes described in Fig. 4 are all highlighted throughout this article. In the Conclusions and outlook section, we highlight some of the ongoing challenges and limitations in this field, along with some recommendations of emerging directions and alternative strong-field ligand designs that could further advance this research. We expect that research in blue phosphorescence will continue to advance fundamentally and lead to significant developments in applied research in the future.

Blue-emitting iridium(III) complexes

Isocyanides have been widely used in the preparation of blue-phosphorescent Ir(III) complexes,[90–92] with early works focused on using *tert*-butyl isocyanide and 2,6-dimethylphenyl isocyanide.[93–95] With an aim to optimize the blue phosphorescence using this ligand class, our group investigated the effects of aryl isocyanides containing different substituents on the emission profiles and excited-state dynamics of cationic bis-cyclometalated Ir(III) complexes. We studied complexes bearing 2,4-difluorophenylpyridine (F_2ppy) as the cyclometalating ligand to give sky-blue phosphorescence and expanded to other cyclometalating ligands that engender deeper-blue PL.[44,46,47] A subset of these compounds are diagrammed in Fig. 6 and described in this section. The detailed

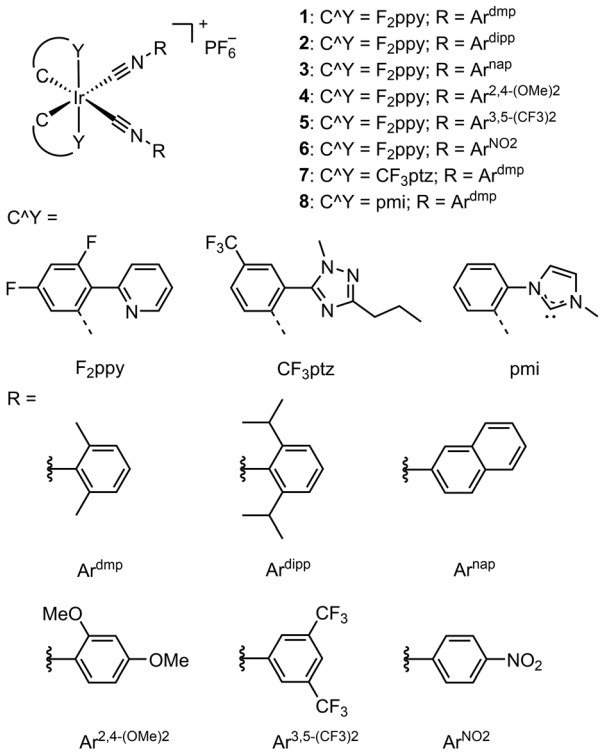

Fig. 6 Cyclometalated Ir(III) complexes containing two isocyanide ancillary ligands.

photophysical properties of all Ir(III) complexes described in this section are provided in Table 1. With some exceptions, the identity of the isocyanide (CNR) has subtle effects on the spectral profile and decay dynamics of the Ir(III) complexes.

Most of the F_2ppy complexes luminesce in the sky-blue region, except for **3** where the phosphorescence originates from a triplet state localized on the naphthyl isocyanide, and **6** where the nitro group quenches luminescence. In the sky-blue emitters, 0–0 transition wavelengths (λ_{0-0}) occur between 417–456 nm. Complex **1** has a Φ_{PL} of 0.37 (recorded in degassed CH_2Cl_2 solution), with k_r and k_{nr} of 9.1×10^3 s^{-1} and 1.5×10^4 s^{-1}, respectively. Augmenting the steric profile of the isocyanide (**2**) decreases Φ_{PL} and k_r slightly, while k_{nr} remains the same. In complex **3**, where the lowest-energy excited state is localized on the naphthyl isocyanide, a low Φ_{PL} of 0.016 was observed. Tuning the electronic profile of the isocyanide (**4** and **5**) led to increases in k_r that resulted in methoxy-substituted **4** having a substantially higher quantum yield. Complexes **7** and **8**, with 1,2,4-triazolyl and NHC-based cyclometalating ligands, respectively, luminesce deeper in the blue region than the F_2ppy complexes. In solution their phosphorescence is weak (complex **7**) or non-existent (complex **8**), but they both exhibit appreciable quantum yields when immobilized in poly(methylmethacrylate) (PMMA) films. Because **8** (λ_{0-0} = 376 nm) has much deeper blue PL than **7** (λ_{0-0} = 416 nm), its quantum yield is much lower, likely due to closer proximity of the T_1 and metal-centered states, as outlined in Fig. 3. These works show that isocyanides are effective at promoting moderate to good quantum yields in the sky-blue region, although their effectiveness wanes in the deep-blue analogues studied.

Isocyanides and cyanide can be paired as ancillary ligands to produce charge-neutral, C_1-symmetric bis-cyclometalated iridium complexes. Iridium complexes of this type with luminescence in the blue-green to sky-blue region have previously been studied by Dedeian *et al.*[96] More recently, our group applied this design to six deep blue-emitting Ir(III) compounds with the general formula $Ir(C^Y)_2(CNR)(CN)$, as displayed in Fig. 7.[49] The combination of cyanide and isocyanides in these complexes stabilize the Ir dπ orbitals, resulting in relatively large HOMO–LUMO gaps. When measured in CH_2Cl_2 solution at room temperature, modest Φ_{PL} values were obtained for the triazole-derived complexes (**9–12**), with **12** giving the highest Φ_{PL}. Complex **12** also has a significantly longer lifetime (τ = 31 μs) than the rest, which we attributed to the larger singlet–triplet gap that led to weaker SOC. All these complexes phosphoresce in the deep-blue region, with **9–11** having CIEy < 0.15, while **13** and **14** bearing NHC-based cyclometalating ligands having shorter-wavelength PL and CIEy < 0.1. Due to the deeper-blue emission, the NHC compounds were not emissive in solution at room temperature, but all are emissive when doped into PMMA at 2 wt%. In this medium, complex **14** has a Φ_{PL} value of 0.22, which is respectable among iridium complexes that luminesce in the extreme deep-blue region. This combination of these ancillary ligands has been shown to effectively raise the energy of deleterious ^{3}MC states and reduce the nonradiative decay.

Coordination of Lewis acids to cyanide increases its π-accepting ability, resulting in an additional stabilization of the metal-centered HOMO energy levels. Complexes bearing cyanide or isocyanoborate paired with isocyanide have been studied by Ko and co-workers,[97] whereas di(isocyanoborate) structures were also reported by Wenger and colleagues.[98] Four representative complexes of these types are displayed in Fig. 8. In solution at room temperature, complex **16** with the $CNB(C_6F_5)_3$ moiety emits in the sky-blue region with a quantum yield of 0.61, a significant improvement when compared to its cyano precursor **15** (Φ_{PL} = 0.44). A very slight blue-shift in emission was also observed. Similarly, complex **18** has a higher Φ_{PL} than its precursor **17**, with Φ_{PL} of 0.87 and 0.64, respectively. There was, however, a more sizeable 20 nm blue shift of the emission maximum after incorporating $B(C_6F_5)_3$ in this case. A significantly longer τ was also obtained in **18**, which the authors attributed to the increased triplet intraligand (^{3}IL) character in the emissive state. The photostability of complex **18** was studied to determine its robustness under visible light radiation. Photodegradation of **18** was observed by NMR analysis after irradiating a pure solution for 60 min. However, the complex remained intact for up to 45 min under the same irradiation conditions but in the presence of norbornadiene as a triplet acceptor.

The strong σ-donating ability of N-heterocyclic carbenes (NHCs) makes them commonly used in coordination chemistry[99–101] and also an attractive ligand class to support blue-phosphorescent Ir(III) complexes,[102–105] with some representative examples shown in Fig. 9. Zuo and colleagues studied neutral bis-cyclometalated Ir(III) complexes bearing a single NHC as a second cyclometalating ligand.[106] They showed that modifying the electronic

Table 1 Summary of emission photophysical properties of blue-phosphorescent Ir(III) complexes

		Photoluminescence properties							
	Ancillary ligand(s)	λ/nm CH_2Cl_2[a]	λ/nm PMMA[c]	(CIEx, CIEy)	Φ_{PL} CH_2Cl_2	Φ_{PL} PMMA[c]	τ/μs CH_2Cl_2	τ/μs PMMA[c]	Ref.
1	Bis(isocyanide)	417, 447	[f]	[f]	0.37	[f]	41	[f]	44
2	Bis(isocyanide)	417, 447	[f]	[f]	0.28	[f]	41	[f]	44
3	Bis(isocyanide)	456, 489, 527, 569	[f]	[f]	0.016	[f]	17, 0.4	[f]	44
4	Bis(isocyanide)	440, 470	438, 468	[f]	0.50	0.88	35	34	46,109
5	Bis(isocyanide)	438, 468	[f]	[f]	0.39	[f]	27	[f]	46
6	Bis(isocyanide)	[b]	[b]	[f]	[b]	[b]	[b]	[f]	46
7	Bis(isocyanide)	415, 444, 472, 512	416, 443, 471, 507	(0.16, 0.09)	0.13	0.49	22	[f]	47
8	Bis(isocyanide)	[b]	376, 399, 414	(0.17, 0.09)	[b]	0.14	[b]	[f]	47
9	Isocyanide + cyanide	411, 437, 464, 495	413, 438, 465, 503	(0.16, 0.13)	0.047	0.14	6.4	[f]	49
10	Isocyanide + cyanide	418, 445, 472, 508	419, 446, 473, 513	(0.16, 0.14)	0.090	0.23	7.6	[f]	49
11	Isocyanide + cyanide	417, 444, 472, 507	417, 444, 472, 507	(0.16, 0.14)	0.064	0.28	4.0	[f]	49
12	Isocyanide + cyanide	432, 462, 484	429, 457, 473	(0.19, 0.24)	0.17	0.38	31	[f]	49
13	Isocyanide + cyanide	[b]	379, 402, 421	(0.16, 0.08)	[b]	0.074	[b]	[f]	49
14	Isocyanide + cyanide	[b]	387, 408, 431	(0.16, 0.06)	[b]	0.22	[b]	[f]	49
15	Isocyanide + cyanide	440, 470	[f]	[f]	0.44	[f]	11	[f]	97
16	Isocyanide + isocyanoborate	438, 467	[f]	[f]	0.61	[f]	32	[f]	97
17	Dicyanide	448[e]	[f]	[f]	0.87[f]	[f]	13[f]	[f]	98
18	Isocyanoborate	468[e]	[f]	[f]	0.64[f]	[f]	2.8[f]	[f]	98
19	Cyclometalated NHC	465, 485	[f]	[f]	0.51	[f]	1.9	[f]	106
20	Pyridyl-NHC	451, 480	452, 480[d]	[f]	0.016	0.44[d]	0.14	3.8[d]	107
21	Chelating bis(NHC)	454, 482	454, 481[d]	[f]	0.36	0.58[d]	3.1	3.2[d]	107
22	NHC + cyanide	386, 408	385, 407	(0.16, 0.04)	0.14	0.56	1.7	7.6	108
23	Cyclometalated ADC	498	492	[f]	0.22	0.79	0.90	1.5	50
24	Cyclometalated ADC	[b]	418	(0.16, 0.07)	[b]	0.13	[b]	6.1	51
25	Cyclometalated ADC	420	418	(0.16, 0.10)	0.013	0.31	[f]	1.8	51
26	Cyclometalated ADC	511	459	(0.16, 0.18)	0.39	0.48	[f]	0.85	51
27	Chugaev dicarbene	453, 474, 498	452, 477	[f]	0.044	0.56	0.63	2.2	45,109
28	Chugaev dicarbene	449, 473, 495	[f]	[f]	0.010	[f]	0.42	[f]	45
29	Chugaev dicarbene	[b]	[f]	[f]	[b]	[f]	[b]	[f]	45
30	Chugaev dicarbene (protonated)	442, 471	445, 472	[f]	0.078	0.68	0.97	6.3	45,109
31	Chugaev dicarbene (protonated)	442, 471	[f]	[f]	0.023	[f]	0.42	[f]	45
32	Chugaev dicarbene (protonated)	[b]	[f]	[f]	[b]	[f]	[b]	[f]	45
33	Isocyanide + cyanamido	449, 476	449, 476	[f]	0.02	0.36	0.40	[f]	52
34	Isocyanide + *C*-tetrazolate	448, 476	448, 475	[f]	0.81	0.35	10	[f]	52
35	ADC + *N*-tetrazolate	455, 481	457, 482	[f]	0.03	0.39	17	[f]	52

[a] Recorded in CH_2Cl_2 at room temperature, unless otherwise noted. [b] Nonemissive. [c] Recorded in PMMA film (2 wt%) at room temperature unless otherwise noted. [d] Recorded in PMMA film (1 wt%) at room temperature. [e] Recorded in CH_3CN at RT. [f] Not reported.

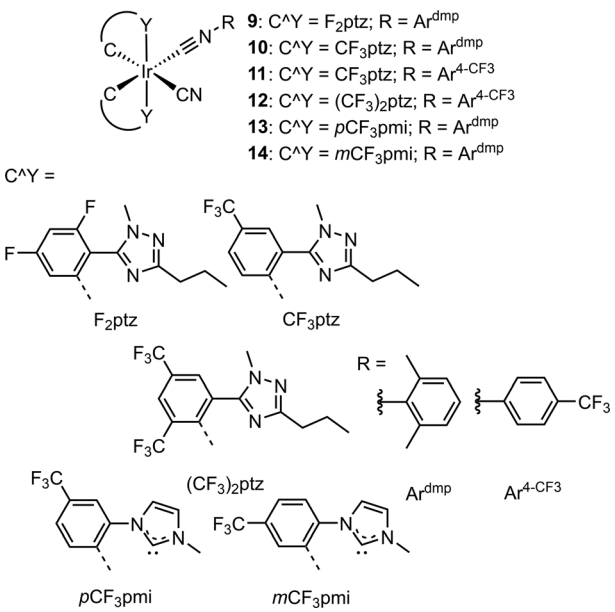

Fig. 7 Cyclometalated Ir(III) complexes containing one isocyanide and one cyanide as ancillary ligands.

characteristics or conjugation of the NHC can tune the HOMO composition and the PL profile of the Ir(III) complexes. Complex **19**, an example which phosphoresced in the sky-blue region, gave a quantum yield of 0.51 with λ_{0-0} = 465 nm when measured in CH_2Cl_2 solution at room temperature. Baranoff and co-workers investigated cationic iridium complexes with chelating NHC-based ancillary ligands, with two representative sky blue-emitting complexes **20** and **21** described here.[107] In contrast to Zuo's work, the NHCs ligands had subtle influences on the emission properties of these complexes. Time-dependent density functional theory (TD-DFT) calculations failed to locate a ^{3}MC state in **21**, which explained the high Φ_{PL} value when measured in CH_2Cl_2 at room temperature. NHCs can also be combined with other monodentate ancillary ligands to support Ir(III) emitters. A ligand set consisting of a tridentate pincer di-NHC ligand, a cyclometalated NHC, and a cyanide ligand was studied by Che and colleagues.[108] The phosphorescence profile was determined by the identity of the bidentate cyclometalating ligand. This strategy has been shown to effectively destabilize the deleterious ^{3}MC states to improve quantum yield in the blue- and deep blue-emitting complexes. For example, complex **22** (λ_{0-0} = 385 nm) gave an extraordinarily high quantum yield of

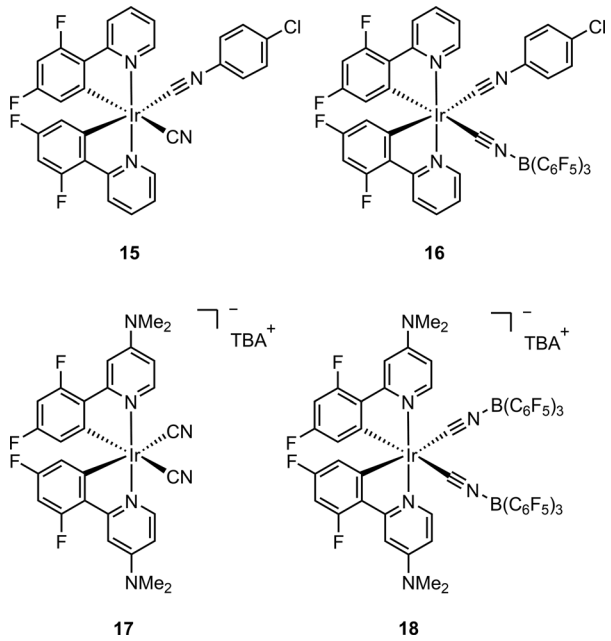

Fig. 8 Some other types of cyclometalated Ir(III) complexes supported by cyanide ligands.

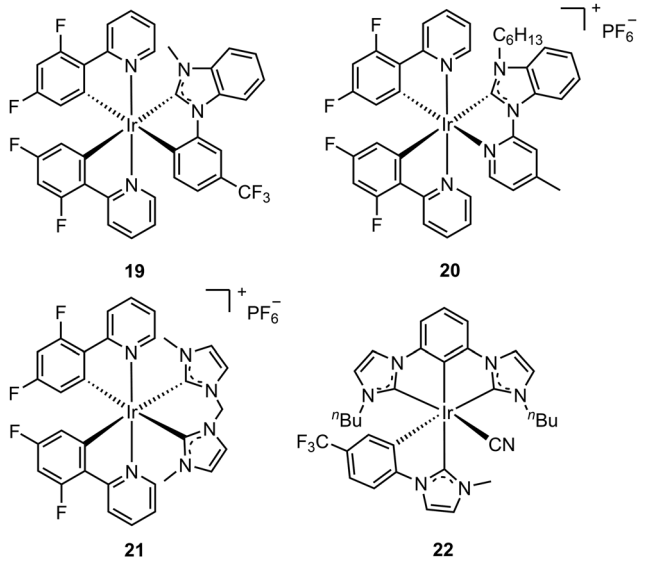

Fig. 9 Representative blue-emitting Ir(III) complexes supported by NHC ancillary ligands.

0.56 when measured in PMMA thin film. Additionally, **22** also showed good thermal stability with only 2 wt% loss at temperatures higher than 350 °C, determined by thermogravimetric analysis and differential scanning calorimetry experiments.

Our group recognized the potential of using acyclic diaminocarbenes to support blue-emitting iridium complexes. As stronger donors than NHCs, the ADC ligands could destabilize the ^{3}MC states to an even greater extent. We introduced ADCs into cyclometalated iridium complexes by adding amine nucleophiles to isocyanide precursors. Nucleophilic addition was accompanied by cyclometallation of the aryl group on the isocyanide, producing tris-chelated products (Scheme 2).[50,51] Complex **23**, with λ_{0-0} = 456 nm (recorded in CH_2Cl_2/toluene at 77 K), has a Φ_{PL} of 0.79 when measured in PMMA film at room temperature, which was among the highest Φ_{PL} obtained for sky-blue Ir(III) phosphors. Moving to the deeper-blue region, compounds **24** and **25** exhibit Φ_{PL} of 0.13 and 0.31 in thin film, respectively. The emission of **26** red shifts to the sky-blue region due to the fused pyridyl ring in the ADC ligand, with Φ_{PL} = 0.48. The lifetimes of all complexes were in the microsecond range, appropriate for OLED device applications. Density functional theory (DFT) calculations were conducted, suggesting that there was minimal triplet-state spin density on the ADC ligands despite their significant contribution to the LUMO. All four complexes **23**–**26** are air stable. The photostability of complex **23** was investigated by irradiating a CH_2Cl_2 solution with a 34 W blue LED for 2.5 h. Under these conditions, the emission intensity of **23** diminished slowly and its final normalized PL spectrum overlaid perfectly with the initial spectrum. The results suggested that there was some photobleaching of **23** but the decomposition products were not luminescent and did not affect the emission profile.

We also prepared Ir(III) complexes supported by chelating di-ADC ligands. Treating bis(isocyanide) complexes with hydrazine afforded neutral "Chuagaev-type" carbene complexes (**27**, **28**, and **29**), and further treatment with HBF_4 gave cationic dicarbene products **30**, **31**, and **32** (Scheme 3).[45] The electron-withdrawing substituents on the isocyanides were critical for promoting the reactivity. In general, the protonated complexes are more strongly luminescent, with roughly two-fold higher Φ_{PL} when measured in CH_2Cl_2 solution at room temperature. Compound **30** has the highest Φ_{PL}, measured to be 0.078 in solution[45] and 0.68 in PMMA film.[109] The PL in **29** and **32** is completely quenched, as often observed in phosphorescent complexes containing nitro groups. The emission profiles of neutral analogues **27** and **28** were significantly temperature-dependent, indicative of thermally accessible excited states involving the dicarbene moieties. In contrast, the low-temperature and room-temperature emission

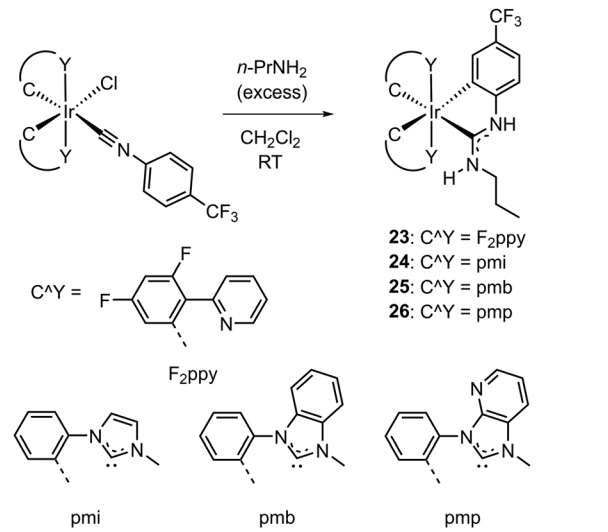

Scheme 2 Cyclometalated Ir(III) complexes supported by ADC ancillary ligands.

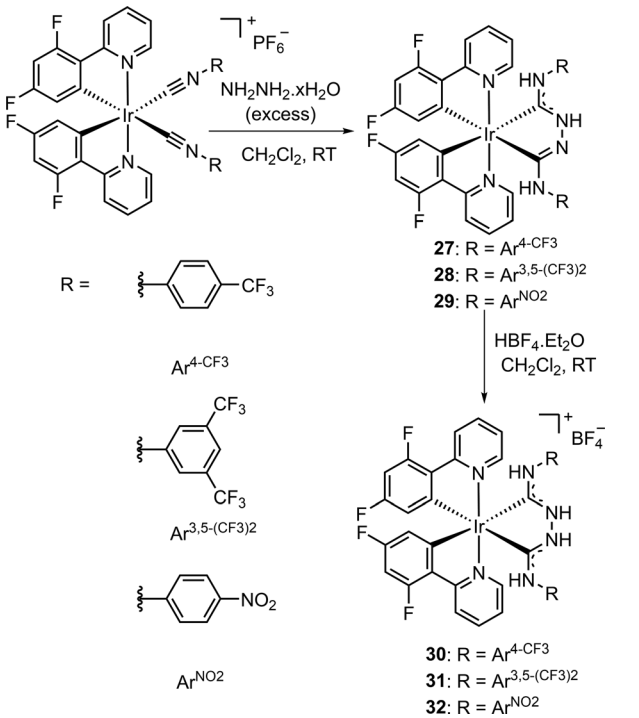

Scheme 3 Cyclometalated Ir(III) complexes with chelating dicarbene ancillary ligands.

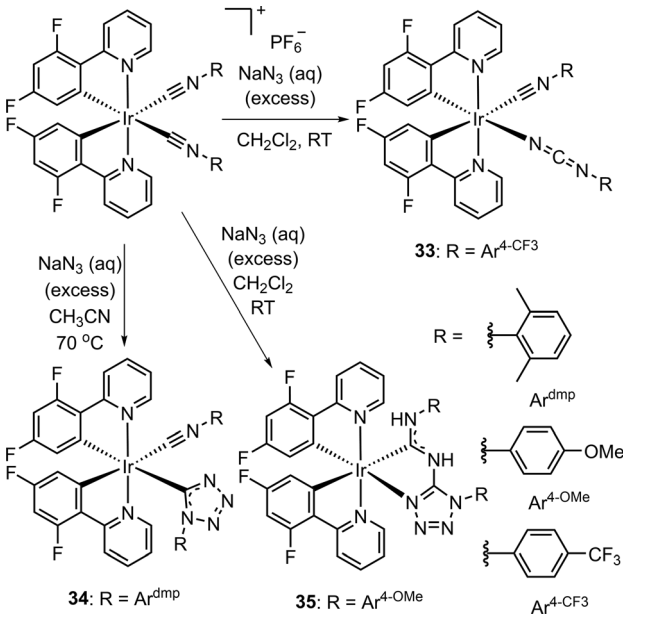

Scheme 4 Different products from reactions between bis(isocyanide) cyclometalated Ir(III) complexes with sodium azide.

spectra of **30** and **31** were very similar, suggesting a more straightforward excited-state landscape with the T_1 state being primarily C^N-ligand localized (^{3}LC) in nature.

In addition to nucleophilic addition of amines or hydrazine, coordinated isocyanides are also known to undergo (3+2) cycloaddition reactions with 1,3-dipoles.[110] Along these lines, our group studied the post-synthetic modification of bis(isocyanide) Ir(III) complexes by reaction with the azide anion, N_3^-.[52] Depending on the functional groups on the isocyanides, different products were obtained. Three examples are shown in Scheme 4, all of which include the cyclometalating ligand F_2ppy to engender sky-blue phosphorescence. Complex **33** forms by expulsion of N_2 after (3+2) cycloaddition, leaving a cyanamido ligand, compound **34** represents the direct (3+2) C-bound tetrazolato product, and complex **35**, which has a chelating *N*-tetrazolato-ADC ligand, forms *via* intramolecular coupling and rearrangement of a tetrazolato and cyanamido. These structures would not be easily accessible by traditional organometallic synthesis. The three complexes phosphoresce in the sky-blue region, with Φ_{PL} in the range of 0.35–0.39 when measured in PMMA film. In CH_2Cl_2 solution at room temperature, **34** has an exceptionally high Φ_{PL} of 0.81. The azide addition results in increased k_r values and slight red shifts of the PL spectra compared to the precursor bis(isocyanide) complexes.

Blue-phosphorescent platinum(II) complexes

Similar to bis(isocyanide) cyclometalated Ir(III) emitters, cyclometalated Pt(II) complexes supported by two isocyanides have been studied in the context of blue phosphorescence. Sicilia and colleagues studied blue-emitting cationic cyclometalated Pt(II) complexes containing two isocyanide ancillary ligands (Fig. 10).[111] The detailed photophysical properties of Pt(II) complexes in this section are given in Table 2. In addition to affecting the excited-state dynamics, the isocyanides also have subtle effects on the emission profiles. All complexes luminesce in the sky-blue region, with the PL assigned to mixed ligand-to-ligand charge transfer (^{3}LL′CT) [π(NHC) → π*(CNR)]/ligand-to-metal charge transfer (^{3}LMCT) [π(NHC) → 5d(Pt)]. The PL bands of **37** and **39** are red-shifted compared to those of **36** and **38**. At higher concentration in solution, additional featureless low-energy bands appear, indicating emission from aggregates. In the solid state at room temperature, compound **36** bearing the more electron-rich isocyanide CN^{t}Bu gives the highest quantum yield at 0.41, while the Φ_{PL} of the remaining complexes ranged from 0.15–0.21.

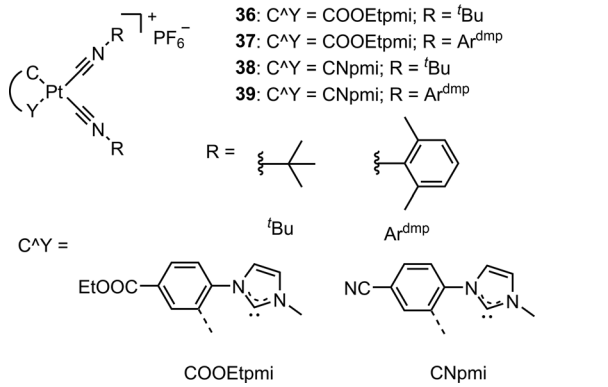

Fig. 10 Cyclometalated Pt(II) complexes supported by isocyanide ligands.

Table 2 Summary of emission photophysical properties of blue-phosphorescent Pt(II) complexes

		Photoluminescence properties							
	Ancillary ligand(s)	λ/nm CH_2Cl_2[a]	λ/nm PMMA[c]	(CIEx, CIEy)	Φ_{PL} CH_2Cl_2	Φ_{PL} PMMA[c]	τ/μs CH_2Cl_2	τ/μs PMMA[c]	Ref.
36	Bis(isocyanide)	455, 486, 520[d]	455, 483, 513, 550[e]	[f]	[b]	0.41[e]	26.5[d]	19.5[e]	111
37	Bis(isocyanide)	464, 495, 531, 600[d]	464, 492, 528, 567[e]	[f]	[b]	0.15[e]	14.5[d]	5.1[e]	111
38	Bis(isocyanide)	451, 482, 517[d]	449, 477, 510, 550[e]	[f]	[b]	0.17[e]	25.0[d]	4.5[e]	111
39	Bis(isocyanide)	461, 494, 529, 569[d]	458, 488, 520, 570[e]	[f]	[b]	0.21[e]	18.0[d]	2.3[e]	111
40	Bis(isocyanide)	430	430	(0.16, 0.11)	[f]	0.014	[f]	2.8	65
41	Bis(isocyanide)	430	430	(0.16, 0.11)	[f]	0.018	[f]	1.5	65
42	Bis(isocyanide)	[b]	435	(0.16, 0.10)	[b]	0.058	[b]	2.8	65
43	Bis(isocyanide)	433, 452, 465, 476[d]	437, 457, 477	(0.17, 0.15)	[f]	0.029	[f]	8.2	66
44	Bis(isocyanide)	437, 464, 480[d]	444, 469	(0.16, 0.18)	[f]	0.12	[f]	3.7	66
45	Bis(isocyanide)	[f]	518, 552	[f]	[f]	0.21	[f]	85	67
46	Di-cyanide	[b]	430, 455, 481[e]	[f]	[b]	0.69[e]	[b]	5.3[e]	114
47	Di-cyanide	445, 462	452, 473[e]	[f]	[f]	0.12[e]	[f]	137[e]	115
48	Cyanide	438, 467, 500	440, 468, 572	[f]	0.009	0.65	<0.1	3.5	116
49	Isocyanoborate	440, 469, 502	442, 470, 500	[f]	0.033	0.75	0.4	8.0	116
50	Chelating bis(NHC)	[b]	422, 444, 470[e]	[f]	[b]	1.0[e]	[b]	33[e]	122
51	Chelating bis(NHC)	[b]	486, 409, 434, 458[e]	[f]	[b]	0.94[e]	[b]	13[e]	122
52	bis(NHC) (*cis*)	432, 465	425, 447[h]	[f]	0.009	0.61[g]	0.24	[f]	123
53	Di-NHC (*trans*)	439, 461	430, 451[h]	[f]	0.010	0.45[g]	3.6	[f]	123
54	ADC + isocyanide	428	428	(0.16, 0.11)	[f]	0.23	[f]	10	65
55	ADC + isocyanide	430	430	(0.16, 0.10)	[f]	0.15	[f]	11	65
56	ADC + isocyanide	425, 445, 455, 467[d]	432, 453, 472	(0.16, 0.15)	[f]	0.16	[f]	14	66
57	ADC + isocyanide	438, 464, 469, 472[d]	447, 474	(0.17, 0.22)	[f]	0.31	[f]	11	66
58	Bis(ADC) (*trans*)	439	440	(0.14, 0.13)	0.07	0.43	8.8	35	68
59	Bis(ADC) (*trans*)	439, 460	437	(0.14, 0.13)	0.01	0.30	1.3	45	68
60	Bis(ADC) (*trans*)	440, 464	438	(0.14, 0.13)	0.02	0.35	2.1	55	68
61	Bis(ADC) (*trans*)	[b]	433	(0.15, 0.16)	[b]	0.45	[b]	18	68
62	Bis(isocyanide)	[f]	467, 499	(0.26, 0.44)	[f]	0.21	[f]	37	64
63	Bis(isocyanide)	[f]	434, 459	(0.17, 0.18)	[f]	0.08	[f]	22	64
64	ADC + isocyanide	[f]	454, 486	(0.19, 0.33)	[f]	0.56	[f]	68	64
65	ADC + isocyanide	[f]	415, 440	(0.16, 0.11)	[f]	0.15	[f]	31	64
66	ADC + cyanide	456[h]	455[h]	(0.18, 0.33)	0.10	0.67	1.2	14	63
67	ADC + cyanide	[b]	415[h]	(0.15, 0.09)	[b]	0.23	[b]	4.6	63
68	ADC + isocyanoborate	456[h]	453[h]	(0.22, 0.37)	0.13	0.75	7.7	30	63
69	ADC + isocyanoborate	[b]	419[h]	(0.15, 0.10)	[b]	0.40	[b]	11	63

[a] Recorded in CH_2Cl_2 at room temperature, unless otherwise noted. [b] Nonemissive. [c] Recorded in PMMA film (2 wt%) at room temperature, unless otherwise noted. [d] Recorded in CH_2Cl_2 at 77 K. [e] Measured in solid state at room temperature. [f] Not reported. [g] Recorded in PMMA film (10 wt%) at room temperature. [h] 0–0 transition wavelength (λ_{0-0}).

In addition to cyclometalating ligands, aryl acetylides have emerged as a common class of chromophoric ligands, offering advantages in the form of readily tunable PL wavelengths with sharp bands. Our group has used isocyanide ligands to support bis(acetylide) Pt(II) complexes, with some examples displayed in Fig. 11.[65–67] The identities of the isocyanides generally have subtle effects on the spectral profile but could affect the excited-state dynamics. We also incorporated electronically modifying substituents or increased the conjugation of the acetylide ligands to examine their influences on the emission wavelengths. In CH_2Cl_2 solution at room temperature, complexes with the unsubstituted phenyl acetylide (**40**–**42**) phosphoresce in the deep-blue region with λ_{0-0} near 430 nm and CIEy < 0.15. Compound **42** (Φ_{PL} = 0.058) containing the aromatic isocyanide $CNAr^{dmp}$ has a higher quantum yield than **40** and **41** (Φ_{PL} = 0.014 and 0.018, respectively). The lowest k_{nr} value was also obtained in **42** at 3.3 × 10^5 s^{-1}. Electron-donating or electron-withdrawing substituents on the acetylides cause red shifts of the PL in **43** and **44**. Complex **45** with the π-extended acetylide shows a further red shift, resulting in

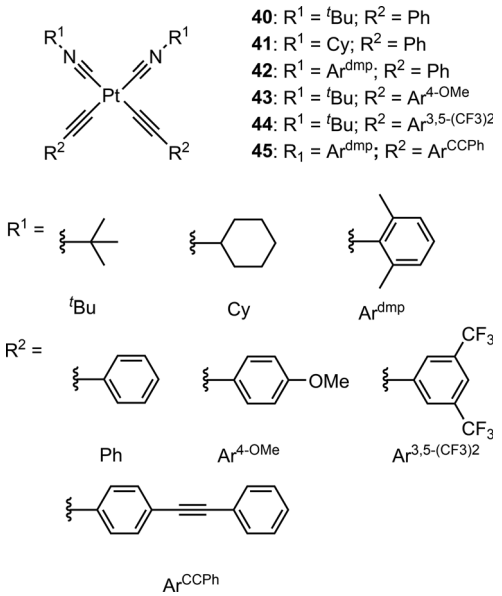

Fig. 11 Acetylide Pt(II) complexes bearing two isocyanide ancillary ligands.

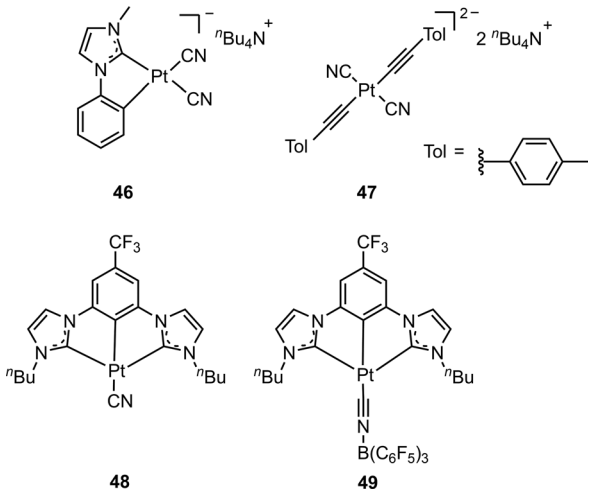

Fig. 12 Representative examples of blue-emitting Pt(II) complexes supported by cyanide.

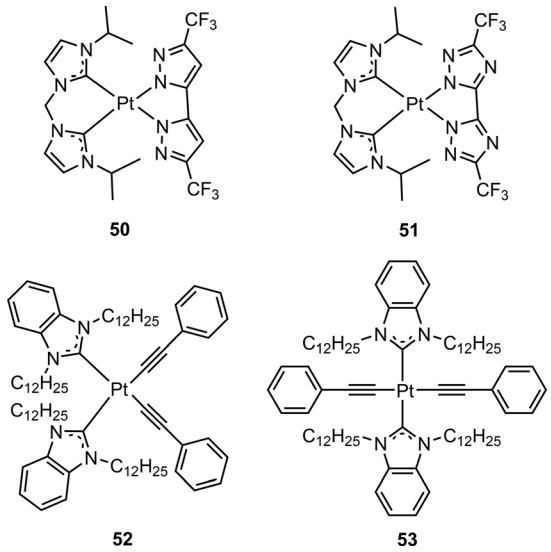

Fig. 13 Representative examples of blue-emitting Pt(II) complexes supported by NHC ligands.

green emission. Interestingly, k_r was improved in complexes bearing electron-withdrawing groups on the acetylides.

Owing to the strong σ-donating ability and π-acidity, cyanide and its Lewis acid-bound derivatives have been used in designing blue-phosphorescent Pt(II) complexes,[112,113] with four representative examples depicted in Fig. 12. Kato and colleagues studied cyclometalated Pt complexes supported by two cyanide ligands.[114] Complex **46** was not luminescent in solution at room temperature but exhibited deep-blue PL in the solid state from a triplet state involving the cyclometalating ligand, giving very high Φ_{PL} values of 0.69 and 0.95 at room temperature and 77 K, respectively. The dianionic compound **47** with the chromophoric acetylide ligand, reported by Sanchez and co-workers,[115] is weakly emissive in solution at room temperature. A modest quantum yield (Φ_{PL} = 0.12) was obtained when measured in solid state, with λ_{0-0} = 452 nm. The authors assigned the emission to the acetylide intraligand transitions. Additionally, **47** showed good stability in solution and in solid state. NHC-based pincer-type Pt(II) complexes bearing monodentate cyanide or isocyanoborate as ancillary ligands were investigated by Che and colleagues.[116] These ligand combinations effectively destabilize the ^{3}MC states, with **48** and **49** giving exceptionally high Φ_{PL} of 0.76 and 0.80 in PMMA thin film, respectively. The luminescence occurs in the sky-blue region, resulting from predominantly a ^{3}IL state localized on the NHC pincer ligand with minor contribution from a ^{3}MLCT state. In CH_2Cl_2 solution, **49** has a Φ_{PL} roughly seven-fold higher than **48**, suggesting a larger d-orbital splitting on account of the more π-acidic isocyanoborate. Complex **48** is prone to excimer formation in solution and PMMA film at high concentrations, whereas the bulky borane moiety ($B(C_6F_5)_3$) in **49** inhibits excimer formation. Both complexes **48** and **49** are air-stable.

N-Heterocyclic carbenes have been extensively used to support blue-phosphorescent Pt(II) complexes.[78,79,117–121] Some representative structures are displayed in Fig. 13. Lee and co-workers investigated Pt(II) complexes containing dianionic azolate chelates and dicarbene chelates,[122] with complexes **50** and **51** giving near-unity Φ_{PL} in solid state with λ_{0-0} = 422 and 386 nm, respectively. TD-DFT calculations showed that the PL in solid state originated from a mixture of $^3(\pi_{N\hat{}N} \rightarrow \pi^*_{C\hat{}C})$, $^3(\pi_{N\hat{}N} \rightarrow Pt(6p))$, and $^3(\pi_{N\hat{}N} \rightarrow \pi^*_{N\hat{}N})$ transitions, indicating that the dicarbene ligands not only influence the excited-state dynamics but also play a key role in the emissive excited states. The blue shift in **51** was attributed to the destabilization of the excited states caused by the stronger electron-withdrawing properties of the bitriazolate chelate compared to the bipyrazole in **50**. The two complexes were, however, not luminescent in solution. Venkatesan and co-workers studied bis(acetylide) Pt(II) complexes supported by two NHC ancillary ligands,[123] and Schanze's group has researched related compounds in the context of blue OLEDs.[78,79,118,119,121] As representative examples, Fig. 13 depicts both *cis* (**52**) and *trans* (**53**) isomers of the same complex, both of which were obtained and characterized. In CH_2Cl_2 solution at room temperature, the two isomers phosphoresce in the blue region, and the PL maximum of **53** is slightly red-shifted compared to **52**. In the solid state, this red shift is more significant with λ_{0-0} = 443 and 430 nm for **53** and **52**, respectively. The *cis* complex has a slightly higher quantum yield (Φ_{PL} = 0.61) than the *trans* isomer (Φ_{PL} = 0.45), when measured in PMMA at 10 wt%. DFT and TD-DFT calculations suggested that the emission can be ascribed to the metal-perturbed ^{3}IL state localized on the acetylide ligands, with a small contribution from ^{3}MLCT.

Again, motivated by their stronger σ-donor capabilities compared to NHCs, our group has extensively studied blue-emitting Pt(II) complexes supported by ADCs. One synthetic advantage we have found with Pt(II) ADC compounds, largely due to their square planar geometry, is more facile nucleophilic addition of amine nucleophiles to isocyanide precursors. Unlike bis-cyclometalated iridium complexes, where unhindered aryl isocyanides with electron-withdrawing groups are required, we have faced no such limitation with Pt(II) complexes. This has enabled us to rapidly explore a few classes of luminescent platinum complexes supported by ADCs, as described in this section. And, in work that is ongoing, we can more extensively study

the synthetic scope and photophysical effects of different substituents on the ADC that originate from the isocyanide or amine nucleophile.

We initially aimed to introduce two ADC ligands onto *cis*-bis(acetylide) bis(isocyanide) Pt(II) complexes by amine nucleophilic addition, using **40–45** (Fig. 11) and related complexes as precursors. However, possibly due to the steric constraints or the decreased electrophilicity of the second isocyanide after the addition of the first amine, only one isocyanide is transformed to an ADC to afford mono(ADC) complexes (Scheme 5), even with a large excess of the nucleophile and reaction times of several days.[65,66] The incorporation of ADCs results in significant enhancements in Φ_{PL}, brought on primarily by a substantial reduction in k_{nr} and resulting in a significantly longer τ. In PMMA thin films, complexes **54** (Φ_{PL} = 0.23) and **55** (Φ_{PL} = 0.15) exhibit deep-blue phosphorescence with a 16-fold and nearly three-fold increase in Φ_{PL} compared to their bis(isocyanide) precursors **40** and **42**, respectively. The emissive excited states are mainly localized on the acetylides, originating from a ^{3}LC transition. The ADC ligands have subtle influences on the emission maxima. Complexes with either electron-donating (**56**) or electron-withdrawing (**57**) functional groups on the aryl acetylide also show improved Φ_{PL}. Compared to their unsubstituted analogue **54**, red shifts in the PL spectra are observed, consistent with the case of bis(isocyanide) Pt(II) complexes discussed above.

We later successfully installed two ADC ligands into bis(acetylide) Pt(II) complexes, affording *trans*-bis(ADC) Pt(II) complexes and enabling even greater enhancements in photophysical properties compared to the mono(ADC) complexes.[68] The one-pot reactions involve both nucleophilic addition of amines to isocyanides, with the amine also serving as the base for copper-mediated acetylide transmetallation (Scheme 6). Key to the synthetic success is the use of *trans*-Pt(CNAr)$_2$I$_2$ precursors, which, unlike precursors that involve other halides or alkyl isocyanides, exist exclusively in the *trans* geometry.[124] All complexes phosphoresce in the blue region in PMMA films, with λ_{0-0} between 433–440 nm. Their Φ_{PL} ranges from 0.30 to 0.45. Varying the isocyanide and amine precursors showed that complex **61** with R^1 = Ar$^{4\text{-OMe}}$ (from the isocyanide) and R^2 = Et (from the amine) has a slightly higher quantum yield than **58–60**. In CH_2Cl_2 solution at room temperature, however, only modest Φ_{PL} values were obtained. In comparison with the mono(ADC) complexes, the second ADC on the bis(ADC) Pt(II) complexes further destabilizes the ^{3}MC state, established computationally, which leads to further suppression of k_{nr}. For example, compared to mono(ADC) complex **55**, there is a nearly five-fold decrease in k_{nr} and a three-fold increase in Φ_{PL} in bis(ADC) complex **58**, which has identical ligand substituents. DFT calculations showed that the energy gap between T_1 and ^{3}MC increases by approximately 0.7 eV with each sequential addition of ADC ligands. The thermal stability of complex **58** was evaluated by thermogravimetric analysis, showing that the onset of decomposition occurred at *ca.* 190 °C.

We also investigated cationic cyclometalated Pt(II) complexes supported by ADC ligands (Scheme 7).[64] Similar to the study of *cis*-bis(acetylide) Pt(II) complexes, only mono(ADC) products (**64** and **65**) were obtained by nucleophilic addition of diethylamine. The emissive excited states were localized on the cyclometalating ligands. Complexes **62** and **64** exhibit sky-blue PL, with **64** having Φ_{PL} of 0.56 (measured in PMMA film), a two-fold increase over its precursor **62**. Similarly, the introduction of ADCs in the deep-blue emitting series improved Φ_{PL}

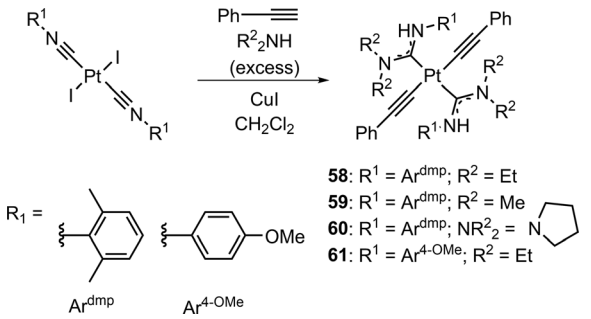

Scheme 6 *Trans*-bis(acetylide) Pt(II) complexes supported by ADC ancillary ligands.

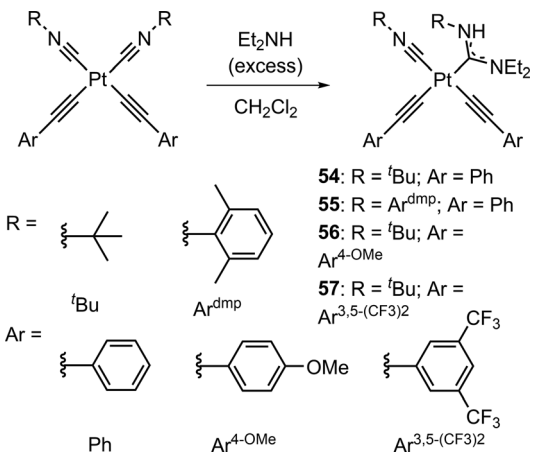

Scheme 5 *Cis*-di(acetylide) Pt(II) complexes supported by ADC ancillary ligands.

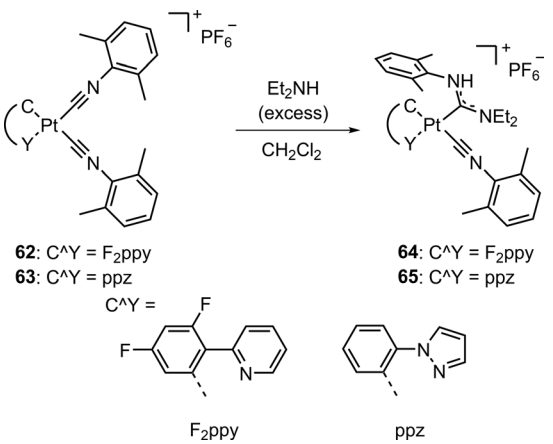

Scheme 7 Cyclometalated Pt(II) complexes containing ADC ancillary ligands.

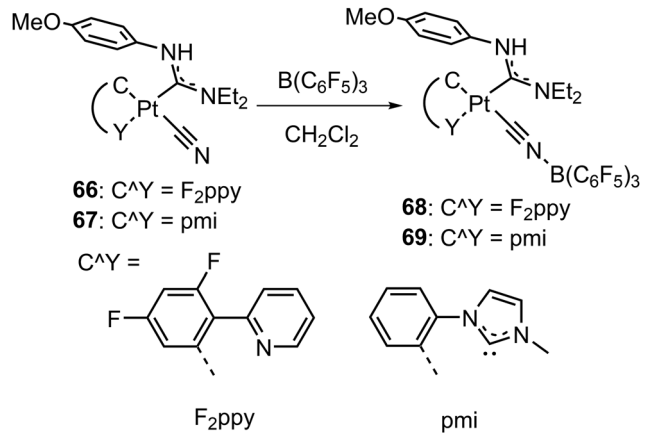

Scheme 8 Cyclometalated Pt(II) complexes containing ADCs paired with cyanide and isocyanoborate ligands.

from 0.08 in complex **63** to 0.15 in **65**. The enhancement of Φ_{PL} was on account of significant decreases in k_{nr} and increases in k_r values. Longer lifetimes and larger HOMO–LUMO gaps were also observed in the ADC complexes. Interestingly, significant blue shifts of emission spectra (13–19 nm) were observed in the ADC complexes relative to their precursors, often difficult to achieve concomitant with improved Φ_{PL}. Other complexes that luminesce outside the blue region were also investigated in this work.

The strategy to combine nucleophilic and electrophilic functionalization strategies on the same platform, which respectively installs ADC and isocyanoborate ancillary ligands, was recently reported by our group (Scheme 8).[63] The combination of these strong-field ancillary ligands effectively raises the energy of the deleterious ^{3}MC states, leading to enhanced photophysical properties in cyclometalated Pt(II) complexes. Complexes **66** and **68** phosphoresce in the sky-blue region with excellent Φ_{PL} of 0.67 and 0.75, respectively, higher than achieved in complex **64**, which is supported by an ADC and an isocyanide. The incorporation of the borane moiety $B(C_6F_5)_3$ increases the π-acidity and ligand-field strength of the cyanide, leading to further suppression of k_{nr}. Likewise, deep-blue emitting complex **69** (λ_{0-0} = 419 nm) shows a nearly two-fold increase in Φ_{PL} of 0.40 when compared to its precursor **67**. In both cases, increases in τ, declines in k_r, and slight shifts of emission maxima were observed.

Conclusions and outlook

As described in the introductory material, the lack of efficient and stable blue-phosphorescent compounds is a problem with immense technological impact, remaining a high-priority R&D target for the color display industry that produces screens for cell phones, TVs, and other consumer products. Addressing this problem requires a wide range of expertise from chemistry and applied fields. Creative ligand designs and innovative organometallic complex structures are needed to achieve breakthrough properties, necessitating the input of the synthetic chemistry community. Contributions from physical and theoretical chemists are needed to reveal the in-depth electronic and photophysical insights that are critical to understanding the relationships between molecular structure and blue-phosphorescent metrics. Finally, as new candidate blue phosphors continue to be developed, applied chemists and engineers will be called upon to test their performance in devices while continuing to innovate device structures and fabrication methods. Thus, we hope readers of this feature article are convinced that the discovery of next-generation blue phosphors is a problem of broad interest to the chemistry community.

The specific chemistry aspects of this feature article focused on key research advances made by our group and several others in blue-emitting Ir(III) and Pt(II) complexes supported by strong-field ancillary ligands. These fundamental investigations towards efficient blue phosphors are relevant to applications across several fields. It was demonstrated throughout this paper that the employment of strong-field ligands, including isocyanides, cyanide, isocyanoborates, N-heterocyclic carbenes, and acyclic diaminocarbenes, can destabilize the thermally accessible nonemissive ^{3}MC states, resulting in enhancements in the photophysical properties and stability of phosphors. Those ligands generally have significant effects on the excited-state dynamics and in some cases could perturb the emission profile (*i.e.* red or blue shifts of emission spectra). Our group has pioneered the use of ADCs as even stronger donors than the universal NHC ligands, producing top-performing blue-emitting Ir(III) and Pt(II) complexes.

Despite the recent advances, many of them summarized here, there remain some key challenges that still need to be addressed. Specific to the research presented here, one limitation we have encountered since shifting much of our focus to blue-phosphorescent platinum complexes is their small k_r values, which leads to long excited-state lifetimes ($\tau > 10$ μs), unsuitable for OLEDs. This class of compounds is desirable for their sharp emission bands, and suppression of k_{nr} by installation of ADCs has been clearly demonstrated, but the lifetimes will need to be substantially reduced if they are to advance towards OLED applications. One strategy we have proposed and have begun investigating is a ''secondary heavy atom'' approach, whereby heavy-metal functional groups are coordinated to the periphery of platinum acetylide complexes, with the goal of augmenting spin–orbit coupling in the excited state and increasing k_r. As a first attempt at realizing this, we recently showed that coordination of the heavy coinage metal Ag^+ to pyridyl-substituted platinum acetylide complexes, supported by isocyanide ancillary ligands, leads to significant increases in k_r and Φ_{PL}.[125] We will continue to explore the versatility of this approach and are interested in extending it to covalently-attached heavy-atom functional groups (*e.g.*, L–Au^+ fragments), which will require significant synthetic advances.

We continue to investigate ADCs as a supporting ligand class for blue-phosphorescent compounds, but there are two major challenges we have identified in our work on this ligand class. The first is a synthetic challenge that is especially pronounced in cyclometalated iridium(III) complexes. Despite having more desirable properties for OLED applications, incorporation of ADCs into cyclometalated iridium complexes is more challenging. This

mainly presents as synthetic incompatibility between certain isocyanides and nucleophiles; for example, all of the cyclometalated iridium(III) ADC complexes we prepared[45,50,51] required unhindered aryl isocyanides with electron-withdrawing groups, and the syntheses were only reliable when unbranched primary amine ($R–NH_2$) nucleophiles were used. This limitation is largely avoided in lower-coordinate Pt(II) complexes but nonetheless does confine the scope of exploration. In addition, there is the burning question of just ''how different'' are ADCs from the more ubiquitous NHCs? In cases where direct comparisons are available in *trans*-Pt(carbene)$_2$(C$\equiv$CPh)$_2$ complexes,[68,78,118] the phosphorescence metrics of the ADC and NHC complexes are broadly similar, although the true impact (or nonimpact) of ADCs will not be realized until thorough device studies are done. To address both challenges, we propose that several other classes of carbene ligands, commonly researched in fundamental organometallic chemistry but rarely applied to photochemistry, could be paradigm shifting. Some carbene ligand classes that are known to be both stronger σ donors and better π acceptors than NHCs are cyclic(alkyl)(amino)carbenes (CAACs), monoamido carbenes (MACs), and diamido carbenes (DACs). There has been a considerable interest in using these ligands for luminescent coinage metal complexes, but the preparation and photophysical study of Ir(III) and Pt(II) complexes, particularly those which luminesce in the deep blue region, have rarely been undertaken.[102] We propose that moving to these alternate carbene structures could avoid the synthetic limitations sometimes faced with ADCs, while perturbing the electronic energy levels to an even greater extent, furthering the goal of suppressing nonradiative decay pathways and improving photostability.

In our opinion, a significant bigger-picture issue, with less of a clear solution, is the poor stability of blue-phosphorescent compounds under device operating conditions. For groups like ours that do fundamental studies on phosphorescence, it is straightforward to evaluate photoluminescence quantum yield and lifetime, and to then claim that a particular compound is desirable for further study as an OLED dopant. And for research groups that fabricate OLEDs, measuring and reporting efficiency metrics is routinely done, with authoritative recommendations that are widely followed to standardize the practice.[126] However, the operational stability and failure mechanisms of devices are less commonly reported on in the academic literature, in part because testing devices until they expire and thoroughly characterizing their degradation pathways[83,84] is unappealing, tedious work. And for groups that do fundamental research on organometallic phosphors, it is difficult to formulate experimental metrics that would lead to predictions about the longevity of a compound in a device. There are simple photostability tests that can be done that consist of photolyzing a compound and monitoring changes in photoluminescence, which we have occasionally performed,[51] but how these results translate to an applied device setting is impossible to predict. Thus, while we do not have a definitive recommendation for how to address this limitation of the field, we do think that it is something the community, including our own group, should think more about and more carefully evaluate when formulating new blue-phosphorescent compounds.

Author contributions

Son N. T. Phan: visualization, writing – original draft, writing – review & editing. Ngoc B. Nguyen: visualization, writing – original draft, writing – review & editing. Thomas S. Teets: funding acquisition, supervision, project administration, writing – review & editing.

Conflicts of interest

There are no conflicts to declare.

Data availability

No primary research results, software or code have been included and no new data were generated or analyzed as part of this review.

Acknowledgements

We acknowledge the National Science Foundation (grant no. CHE-2348784) and the Welch Foundation (grant no. E-1887) for their support of our group's research on blue-phosphorescent organometallic complexes.

Notes and references

1 Z.-J. Yao, Y.-X. Jin, W. Deng and Z.-J. Liu, *Inorg. Chem.*, 2021, **60**, 2756–2763.
2 Y. Niu, F. Zhang, T. Li, Y. Li, H. Han, D. Wei, B. Zhai and B. Wei, *J. Mol. Struct.*, 2024, **1301**, 137355.
3 J. Hu, J. Pei, W. Tang and C. Fan, *J. Am. Soc. Mass Spectrom.*, 2024, **35**, 357–364.
4 S. Mishra and S. Patra, *Dalton Trans.*, 2024, **53**, 8214–8222.
5 D. Gómez De Segura, A. Corral-Zorzano, E. Alcolea, M. T. Moreno and E. Lalinde, *Inorg. Chem.*, 2024, **63**, 1589–1606.
6 M. Benítez, M. L. Buil, M. A. Esteruelas, A. M. López, C. Martín-Escura and E. Oñate, *Inorg. Chem.*, 2024, **63**, 6346–6361.
7 M. Denison, J. J. Ahrens, M. N. Dunbar, H. Warmahaye, A. Majeed, C. Turro, T. A. Kocarek, I. F. Sevrioukova and J. J. Kodanko, *Inorg. Chem.*, 2023, **62**, 3305–3320.
8 W. Li, T. Li, Y. Pan, S. Li, G. Xu, Z. Zhang, H. Liang and F. Yang, *J. Med. Chem.*, 2024, **67**, 3843–3859.
9 N. Kashyap, M. Rabha, S. K. Patra, B. Sen, S. K. Sheet, K. Baruah and S. Khatua, *Cryst. Growth Des.*, 2024, **24**, 3615–3631.
10 Z. Ruan, J. Yang, Y. Li and K. Y. Zhang, *ChemBioChem*, 2024, **25**, e202400094.
11 J. Zhang, Z. Zhang, M. Su, X. Xu, R. Gao, B. Yu and X. Yan, *Inorg. Chem.*, 2024, **63**, 22782–22791.
12 V. Rigolot, C. Simon, A. Bouchet, L. Lancel, V. Di Battista, D. Karpov, B. Vauzeilles, C. Spriet, M. Sliwa, S. Bohic, C. Biot and C. Lion, *RSC Chem. Biol.*, 2025, **6**, 364–375.
13 T. S. Teets, *Photoluminescence*, American Chemical Society, Washington, DC, USA, 2021.
14 J. B. Goodenough, *Phys. Rev.*, 1968, **171**, 466–479.
15 H. Yersin and W. J. Finkenzeller, *Highly Efficient OLEDs with Phosphorescent Materials*, John Wiley & Sons, Ltd, 2007, pp. 1–97.
16 C. M. Marian, *Wiley Interdiscip. Rev.:Comput. Mol. Sci.*, 2012, **2**, 187–203.
17 M. A. Baldo, D. F. O'Brien, Y. You, A. Shoustikov, S. Sibley, M. E. Thompson and S. R. Forrest, *Nature*, 1998, **395**, 151–154.
18 C. Adachi, M. A. Baldo, M. E. Thompson and S. R. Forrest, *J. Appl. Phys.*, 2001, **90**, 5048–5051.
19 V. Pandit, J. Jang, C. S. K. Ranasinghe, P. L. Burn, E. V. Puttock and P. E. Shaw, *J. Mater. Chem. C*, 2024, **12**, 4751–4761.
20 G. Li, L. Ameri, B. Dorame, Z. Zhu and J. Li, *Adv. Funct. Mater.*, 2024, **34**, 2405066.
21 M. A. Baldo, S. Lamansky, P. E. Burrows, M. E. Thompson and S. R. Forrest, *Appl. Phys. Lett.*, 1999, **75**, 4–6.

22 S. Lamansky, P. Djurovich, D. Murphy, F. Abdel-Razzaq, H.-E. Lee, C. Adachi, P. E. Burrows, S. R. Forrest and M. E. Thompson, *J. Am. Chem. Soc.*, 2001, **123**, 4304–4312.
23 K. Tong, C. Wu, Y. Wu, S. Li, Z. Jin, K. Shi, S. Jung, X. Wang, Y. Guan, C. Yang and G. Wei, *Small*, 2024, **20**, 2307500.
24 H.-Y. Li, L. Zhou, M.-Y. Teng, Q.-L. Xu, C. Lin, Y.-X. Zheng, J.-L. Zuo, H.-J. Zhang and X.-Z. You, *J. Mater. Chem. C*, 2013, **1**, 560–565.
25 C. Wu, K. Shi, S. Li, J. Yan, Z.-Q. Feng, K.-N. Tong, S.-W. Zhang, Y. Zhang, D. Zhang, L.-S. Liao, Y. Chi, G. Wei and F. Kang, *EnergyChem*, 2024, **6**, 100120.
26 W.-Q. Zheng, K.-Y. Lu, X.-Q. Gan, H. Zhang, X.-Q. Yan, J.-T. Yu, Y.-F. Wang, X.-G. Wu and W.-G. Zhu, *J. Mater. Chem. C*, 2023, **11**, 4017–4024.
27 T. Fu, S. Cheng, Y. Chen, Y. Chang, X. Jiao, C. Zhang, Q. Xia, Z. Sun and X.-C. Hang, *Adv. Opt. Mater.*, 2024, **12**, 2301321.
28 H. Lee, B. Park, G. R. Han, M. S. Mun, S. Kang, W. P. Hong, H. Y. Oh and T. Kim, *Adv. Mater.*, 2024, **36**, 2409394.
29 E. Longhi and L. De Cola, *Iridium(III) in Optoelectronic and Photonics Applications*, John Wiley & Sons, Ltd, 2017, pp. 205–274.
30 S. Lee and W.-S. Han, *Inorg. Chem. Front.*, 2020, **7**, 2396–2422.
31 T. Maganti and K. Venkatesan, *ChemPlusChem*, 2022, **87**, e202200014.
32 Y. Liu, G. Gahungu, X. Sun, J. Su, X. Qu and Z. Wu, *Dalton Trans.*, 2012, **41**, 7595.
33 M. Samandar Sangari, M. Golbon Haghighi, S. M. Nabavizadeh, A. Pfitzner and M. Rashidi, *New J. Chem.*, 2018, **42**, 8661–8671.
34 S. Baek, S.-Y. Kwak, S.-T. Kim, K. Y. Hwang, H. Koo, W.-J. Son, B. Choi, S. Kim, H. Choi and M.-H. Baik, *Nat. Commun.*, 2020, **11**, 2292.
35 K. A. King, P. J. Spellane and R. J. Watts, *J. Am. Chem. Soc.*, 1985, **107**, 1431–1432.
36 L. Chassot and A. Von Zelewsky, *Inorg. Chem.*, 1987, **26**, 2814–2818.
37 T. Sajoto, P. I. Djurovich, A. Tamayo, M. Yousufuddin, R. Bau, M. E. Thompson, R. J. Holmes and S. R. Forrest, *Inorg. Chem.*, 2005, **44**, 7992–8003.
38 S.-C. Lo, C. P. Shipley, R. N. Bera, R. E. Harding, A. R. Cowley, P. L. Burn and I. D. W. Samuel, *Chem. Mater.*, 2006, **18**, 5119–5129.
39 R. Ragni, E. A. Plummer, K. Brunner, J. W. Hofstraat, F. Babudri, G. M. Farinola, F. Naso and L. De Cola, *J. Mater. Chem.*, 2006, **16**, 1161.
40 J. H. Seo, Y. K. Kim and Y. Ha, *Thin Solid Films*, 2009, **517**, 1807–1810.
41 T. Karatsu, M. Takahashi, S. Yagai and A. Kitamura, *Inorg. Chem.*, 2013, **52**, 12338–12350.
42 A. K. Pal, S. Krotkus, M. Fontani, C. F. R. Mackenzie, D. B. Cordes, A. M. Z. Slawin, I. D. W. Samuel and E. Zysman-Colman, *Adv. Mater.*, 2018, **30**, 1804231.
43 J. Lee, H.-F. Chen, T. Batagoda, C. Coburn, P. I. Djurovich, M. E. Thompson and S. R. Forrest, *Nat. Mater.*, 2016, **15**, 92–98.
44 A. Maity, L. Q. Le, Z. Zhu, J. Bao and T. S. Teets, *Inorg. Chem.*, 2016, **55**, 2299–2308.
45 H. Na, A. Maity, R. Morshed and T. S. Teets, *Organometallics*, 2017, **36**, 2965–2972.
46 H. Na, A. Maity and T. S. Teets, *Dalton Trans.*, 2017, **46**, 5008–5016.
47 L. M. Cañada, J. Kölling and T. S. Teets, *Polyhedron*, 2020, **178**, 114332.
48 C. Jiang, L. M. Cañada, N. B. Nguyen and T. S. Teets, *J. Organomet. Chem.*, 2023, **984**, 122561.
49 L. M. Cañada, J. Kölling, Z. Wen, J. I.-C. Wu and T. S. Teets, *Inorg. Chem.*, 2021, **60**, 6391–6402.
50 H. Na and T. S. Teets, *J. Am. Chem. Soc.*, 2018, **140**, 6353–6360.
51 H. Na, L. M. Cañada, Z. Wen, J. I-Chia Wu and T. S. Teets, *Chem. Sci.*, 2019, **10**, 6254–6260.
52 C. Jiang, L. M. Cañada, N. B. Nguyen, M. D. S. Halamicek, S. H. Nguyen and T. S. Teets, *J. Am. Chem. Soc.*, 2023, **145**, 1227–1235.
53 C.-Y. Kuei, S.-H. Liu, P.-T. Chou, G.-H. Lee and Y. Chi, *Dalton Trans.*, 2016, **45**, 15364–15373.
54 C. Kuei, W. Tsai, B. Tong, M. Jiao, W. Lee, Y. Chi, C. Wu, S. Liu, G. Lee and P. Chou, *Adv. Mater.*, 2016, **28**, 2795–2800.
55 L. Hsu, Q. Liang, Z. Wang, H. Kuo, W. Tai, S. Su, X. Zhou, Y. Yuan and Y. Chi, *Chem. – Eur. J.*, 2019, **25**, 15375–15386.
56 W.-S. Tai, L.-Y. Hsu, W.-Y. Hung, Y.-Y. Chen, C.-L. Ko, X. Zhou, Y. Yuan, A. K.-Y. Jen and Y. Chi, *J. Mater. Chem. C*, 2020, **8**, 13590–13602.
57 L. Yang, F. Okuda, K. Kobayashi, K. Nozaki, Y. Tanabe, Y. Ishii and M. Haga, *Inorg. Chem.*, 2008, **47**, 7154–7165.
58 C. Lin, Y. Chang, J. Hung, C. Lin, Y. Chi, M. Chung, C. Lin, P. Chou, G. Lee, C. Chang and W. Lin, *Angew. Chem., Int. Ed.*, 2011, **50**, 3182–3186.
59 C. Wu, M. Wang, K. Tong, M. Zhang, W. Li, Z. Xu, W. Zhang, Y. Wu, C. Yang, H. Fu, S. S. Chen, M. Ng, M. Tang and G. Wei, *Adv. Opt. Mater.*, 2023, **11**, 2201998.
60 C. Wu, K. Tong, M. Zhang, M. Ng, S. Zhang, W. Cai, S. Jung, Y. Wu, C. Yang, M. Tang and G. Wei, *Adv. Opt. Mater.*, 2022, **10**, 2200356.
61 Y. Yuan, P. Gnanasekaran, Y.-W. Chen, G.-H. Lee, S.-F. Ni, C.-S. Lee and Y. Chi, *Inorg. Chem.*, 2020, **59**, 523–532.
62 Y.-S. Li, J.-L. Liao, K.-T. Lin, W.-Y. Hung, S.-H. Liu, G.-H. Lee, P.-T. Chou and Y. Chi, *Inorg. Chem.*, 2017, **56**, 10054–10060.
63 Y. H. Nguyen, Y. Wu, V. Q. Dang, C. Jiang and T. S. Teets, *J. Am. Chem. Soc.*, 2024, **146**, 9224–9229.
64 Y. H. Nguyen, L. T. M. Dang, M. Cornu, C. Jiang, A. C. Darrow, V. Q. Dang and T. S. Teets, *ACS Appl. Opt. Mater.*, 2024, **2**, 2019–2030.
65 Y. Wu, Z. Wen, J. I. Wu and T. S. Teets, *Chem. – Eur. J.*, 2020, **26**, 16028–16035.
66 Y. H. Nguyen, J. V. Soares, S. H. Nguyen, Y. Wu, J. I. Wu and T. S. Teets, *Inorg. Chem.*, 2022, **61**, 8498–8508.
67 J. C. López-López, Y. H. Nguyen, C. Jiang and T. S. Teets, *Inorg. Chem.*, 2023, **62**, 17843–17850.
68 Y. H. Nguyen, V. Q. Dang, J. V. Soares, J. I. Wu and T. S. Teets, *Chem. Sci.*, 2023, **14**, 4857–4862.
69 X. Zhang, A. M. Wright, N. J. DeYonker, T. K. Hollis, N. I. Hammer, C. E. Webster and E. J. Valente, *Organometallics*, 2012, **31**, 1664–1672.
70 S.-H. Wu, J.-Y. Shao, Z. Zhao, J. Ma, R. Yang, N. Chen, J.-H. Tang, Z. Bian and Y.-W. Zhong, *Organometallics*, 2021, **40**, 156–165.
71 K. Li, Q. Wan, C. Yang, X. Chang, K. Low and C. Che, *Angew. Chem., Int. Ed.*, 2018, **130**, 14325–14329.
72 G. Li, X. Zhao, T. Fleetham, Q. Chen, F. Zhan, J. Zheng, Y.-F. Yang, W. Lou, Y. Yang, K. Fang, Z. Shao, Q. Zhang and Y. She, *Chem. Mater.*, 2020, **32**, 537–548.
73 F. Yu, Y. Sheng, D. Wu, K. Qin, H. Li, G. Xie, Q. Xue, Z. Sun, Z. Lu, H. Ma and X.-C. Hang, *Inorg. Chem.*, 2020, **59**, 14493–14500.
74 P. Pinter, J. Soellner and T. Strassner, *Organometallics*, 2021, **40**, 557–563.
75 K. Lo, G. S. M. Tong, G. Cheng, K. Low and C. Che, *Angew. Chem.*, 2022, **134**, e202115515.
76 R. A. Shilov, I. S. Podkorytov, K. S. Kisel, E. E. Galenko, D. O. Karpitskaya, I. A. Rodionov, J. R. Shakirova and S. P. Tunik, *Inorg. Chem.*, 2024, **63**, 11194–11208.
77 J.-Z. Fu, X. Zhang, J.-Y. Wang, L.-Y. Zhang and Z.-N. Chen, *Inorg. Chem. Commun.*, 2012, **22**, 123–125.
78 J. D. Bullock, S. R. Valandro, A. N. Sulicz, C. J. Zeman, K. A. Abboud and K. S. Schanze, *J. Phys. Chem. A*, 2019, **123**, 9069–9078.
79 R. He, Z. Xu, S. Valandro, H. D. Arman, J. Xue and K. S. Schanze, *ACS Appl. Mater. Interfaces*, 2021, **13**, 5327–5337.
80 C.-Y. Chan, M. Tanaka, H. Nakanotani and C. Adachi, *Nat. Commun.*, 2018, **9**, 5036.
81 M. Zhu and C. Yang, *Chem. Soc. Rev.*, 2013, **42**, 4963.
82 R. Seifert, S. Scholz, B. Lüssem and K. Leo, *Appl. Phys. Lett.*, 2010, **97**, 013308.
83 R. Seifert, I. Rabelo De Moraes, S. Scholz, M. C. Gather, B. Lüssem and K. Leo, *Org. Electron.*, 2013, **14**, 115–123.
84 M. J. Jurow, A. Bossi, P. I. Djurovich and M. E. Thompson, *Chem. Mater.*, 2014, **26**, 6578–6584.
85 J. A. M. Lummiss, C. S. Higman, D. L. Fyson, R. McDonald and D. E. Fogg, *Chem. Sci.*, 2015, **6**, 6739–6746.
86 G. D. Sutton, M. E. Olumba, Y. H. Nguyen and T. S. Teets, *Dalton Trans.*, 2021, **50**, 17851–17863.
87 H. P. DeGroot and T. P. Hanusa, in *Encyclopedia of Inorganic and Bioinorganic Chemistry*, ed. R. A. Scott, Wiley, 2nd edn, 2020, pp. 1–13.
88 M. A. Kinzhalov and K. V. Luzyanin, *Coord. Chem. Rev.*, 2019, **399**, 213014.
89 C. Singh, A. Kumar and H. V. Huynh, *Inorg. Chem.*, 2020, **59**, 8451–8460.
90 A. Giussani, P. Pla, J. M. Junquera-Hernández and E. Ortí, *Dalton Trans.*, 2019, **48**, 9725–9733.
91 A. Baschieri, L. Sambri, A. Mazzanti, A. Carlone, F. Monti and N. Armaroli, *Inorg. Chem.*, 2020, **59**, 16238–16250.
92 F. Monti, A. Baschieri, L. Sambri and N. Armaroli, *Acc. Chem. Res.*, 2021, **54**, 1492–1505.
93 N. M. Shavaleev, F. Monti, R. Scopelliti, A. Baschieri, L. Sambri, N. Armaroli, M. Grätzel and M. K. Nazeeruddin, *Organometallics*, 2013, **32**, 460–467.
94 N. M. Shavaleev, F. Monti, R. Scopelliti, N. Armaroli, M. Grätzel and M. K. Nazeeruddin, *Organometallics*, 2012, **31**, 6288–6296.

95 N. M. Shavaleev, F. Monti, R. D. Costa, R. Scopelliti, H. J. Bolink, E. Ortí, G. Accorsi, N. Armaroli, E. Baranoff, M. Grätzel and M. K. Nazeeruddin, *Inorg. Chem.*, 2012, **51**, 2263–2271.
96 K. Dedeian, J. Shi, E. Forsythe, D. C. Morton and P. Y. Zavalij, *Inorg. Chem.*, 2007, **46**, 1603–1611.
97 K.-C. Chan, W.-K. Chu, S.-M. Yiu and C.-C. Ko, *Dalton Trans.*, 2015, **44**, 15135–15144.
98 L. Schmid, F. Glaser, R. Schaer and O. S. Wenger, *J. Am. Chem. Soc.*, 2022, **144**, 963–976.
99 W. A. Herrmann and C. Köcher, *Angew. Chem., Int. Ed. Engl.*, 1997, **36**, 2162–2187.
100 D. Bourissou, O. Guerret, F. P. Gabbaï and G. Bertrand, *Chem. Rev.*, 2000, **100**, 39–92.
101 H. Amouri, *Chem. Rev.*, 2023, **123**, 230–270.
102 C.-H. Yang, J. Beltran, V. Lemaur, J. Cornil, D. Hartmann, W. Sarfert, R. Fröhlich, C. Bizzarri and L. De Cola, *Inorg. Chem.*, 2010, **49**, 9891–9901.
103 C. Hsieh, F. Wu, C. Fan, M. Huang, K. Lu, P. Chou, Y. O. Yang, S. Wu, I. Chen, S. Chou, K. Wong and C. Cheng, *Chem. – Eur. J.*, 2011, **17**, 9180–9187.
104 H. Kuo, Z. Zhu, C. Lee, Y. Chen, S. Liu, P. Chou, A. K.-Y. Jen and Y. Chi, *Adv. Sci.*, 2018, **5**, 1800846.
105 Z.-L. Zhu, P. Gnanasekaran, J. Yan, Z. Zheng, C.-S. Lee, Y. Chi and X. Zhou, *Inorg. Chem.*, 2022, **61**, 8898–8908.
106 T.-Y. Li, X. Liang, L. Zhou, C. Wu, S. Zhang, X. Liu, G.-Z. Lu, L.-S. Xue, Y.-X. Zheng and J.-L. Zuo, *Inorg. Chem.*, 2015, **54**, 161–173.
107 F. Monti, F. Kessler, M. Delgado, J. Frey, F. Bazzanini, G. Accorsi, N. Armaroli, H. J. Bolink, E. Ortí, R. Scopelliti, Md. K. Nazeeruddin and E. Baranoff, *Inorg. Chem.*, 2013, **52**, 10292–10305.
108 Y. Wu, C. Yang, J. Liu, M. Zhang, W. Liu, W. Li, C. Wu, G. Cheng, Q. Yang, G. Wei and C.-M. Che, *Chem. Sci.*, 2021, **12**, 10165–10178.
109 H. Na, P. Lai, L. M. Cañada and T. S. Teets, *Organometallics*, 2018, **37**, 3269–3277.
110 V. P. Boyarskiy, N. A. Bokach, K. V. Luzyanin and V. Yu Kukushkin, *Chem. Rev.*, 2015, **115**, 2698–2779.
111 S. Fuertes, A. J. Chueca, M. Perálvarez, P. Borja, M. Torrell, J. Carreras and V. Sicilia, *ACS Appl. Mater. Interfaces*, 2016, **8**, 16160–16169.
112 A. F. Rausch, U. V. Monkowius, M. Zabel and H. Yersin, *Inorg. Chem.*, 2010, **49**, 7818–7825.
113 S. Fuertes, A. J. Chueca, A. Martín and V. Sicilia, *J. Organomet. Chem.*, 2019, **889**, 53–61.
114 T. Ogawa, W. M. C. Sameera, D. Saito, M. Yoshida, A. Kobayashi and M. Kato, *Inorg. Chem.*, 2018, **57**, 14086–14096.
115 J. R. Berenguer, J. Fernández, E. Lalinde and S. Sánchez, *Organometallics*, 2013, **32**, 835–845.
116 J. Liu, T.-L. Lam, M.-K. Sit, Q. Wan, C. Yang, G. Cheng and C.-M. Che, *J. Mater. Chem. C*, 2022, **10**, 10271–10283.
117 Y. Zhang, J. A. Garg, C. Michelin, T. Fox, O. Blacque and K. Venkatesan, *Inorg. Chem.*, 2011, **50**, 1220–1228.
118 J. D. Bullock, A. Salehi, C. J. Zeman, K. A. Abboud, F. So and K. S. Schanze, *ACS Appl. Mater. Interfaces*, 2017, **9**, 41111–41114.
119 J. D. Bullock, Z. Xu, S. Valandro, M. Younus, J. Xue and K. S. Schanze, *ACS Appl. Electron. Mater.*, 2020, **2**, 1026–1034.
120 Y. Shen, X. Kong, F. Yang, H.-D. Bian, G. Cheng, T. R. Cook and Y. Zhang, *Inorg. Chem.*, 2022, **61**, 16707–16717.
121 A. A. T. Khan, H. B. Gobeze, T. Islam, H. D. Arman and K. S. Schanze, *Dalton Trans.*, 2023, **52**, 11535–11542.
122 J.-L. Liao, Y. Chi, J.-Y. Wang, Z.-N. Chen, Z.-H. Tsai, W.-Y. Hung, M.-R. Tseng and G.-H. Lee, *Inorg. Chem.*, 2016, **55**, 6394–6404.
123 Y. Zhang, O. Blacque and K. Venkatesan, *Chem. – Eur. J.*, 2013, **19**, 15689–15701.
124 T. Kaharu, T. Tanaka, M. Sawada and S. Takahashi, *J. Mater. Chem.*, 1994, **4**, 859–865.
125 V. Q. Dang, C. Jiang and T. S. Teets, *Chem. Sci.*, 2025, **16**, 7302–7310.
126 S. R. Forrest, D. D. C. Bradley and M. E. Thompson, *Adv. Mater.*, 2003, **15**, 1043–1048.